Vol. 45, No. 1 (2023) 111-120, DOI: 10.24874/ti.1386.10.22.01

Tribology in Industry

www.tribology.rs

RESEARCH

Effect of Filler Materials on Abrasive Wear Performance of Glass/Epoxy Composites

Bheemappa Suresha[a,*], Shivaprakash Vidyashree[a], Harshavardhan Bettegowda[a]

[a]*The National Institute of Engineering, Mysuru, Karnataka, India*

Keywords:

Bidirectional glass-epoxy composites
Ceramic fillers
Three-body abrasive wear
Wear volume
Specific wear rate

* Corresponding author:

B. Suresha
E-mail: sureshab@nie.ac.in

Received: 9 October 2022
Revised: 26 November 2022
Accepted: 21 January 2023

A B S T R A C T

When creating polymer-based composites, plain weave fabrics and micron-sized fillers offer bidirectional strength and reduced voids/inhomogeneity. In the present work, It was investigated how glass fabric reinforced epoxy composite (G-E) performed during three-body abrasive wear with and without ceramic fillers (SiO_2, Al_2O_3, graphite, and fly ash cenospheres). In experiments, loads of 20 N and 40 N were applied at various abrading distances of 500 m, 1000 m, 1500 m, and 2000 m. According to the results of sand abrasive wear test, the specific wear rates of G-E based composites are sensitive to fibre and filler/matrix adhesion. Under all tribo-test settings, the SWR for all particulate G-E composites decreases in the following order: G-E > Gr/G-E > SiO_2/G-E > Al_2O_3/G-E > fly ash cenosphere/G-E. Furthermore, the specific wear rate of the fly ash cenosphere filled G-E composites were found to be lower than the G-E and other filler materials filled G-E composites. There was 38.7% reduction in the specific wear rate at 40 N, 2000 m in fly ash cenosphere filled G-E composite. As per the evidence of scanning electron microscope images of worn-out surfaces, mechanisms such as ploughing, fibre breakage, fibre pull-out, fibre thinning, and a network of microcracks caused the wear in composites.

1. INTRODUCTION

A recent study found that glass fibers have been used as strengthening agent with epoxy matrix material for structural applications [1]. Some advantages include high specific characteristics, low cost, bidirectional strength, and simplicity of handling. They are employed in the building and automotive industries due to its superior mechanical qualities, low cost, and ease of fabrication [2]. Gears, bearings, and sleeves are just a few examples of mechanical components that frequently make use of polymers and their mono and hybrid composites. This is a prominent class of man-made composite materials for tribo-engineering, where tribo-performance in non-lubricated settings is a key material selection characteristic [3].

Fiber and particulate-reinforced epoxy composite materials have suitable tribological characteristics [4–8]. The number of research articles on epoxy as a matrix material with glass fibres and ceramic fillers for improving the qualities in mechanical and abrasion resistance has increased over the past ten years [9-18]. Wind turbine blades were made of polymer composite materials that had glass fibre reinforcement [19].

Table 1. Summary of the wear behaviour of micron sized particulates reinforced composites.

Composite	Fabrication	Loading of filler	Output	Ref.
MoS_2 and Al_2O_3 fillers + CF-epoxy	Hand lay-up	5, and 10 wt. % each	Inclusion of MoS_2 and Al_2O_3 composites separately improved the two-body abrasive wear resistance.	[17]
Graphite and alumina + GF-epoxy	Hand lay-up	2.5, 5 and 7.5 wt. %	Alumina filled GF-epoxy composite enhanced the wear resistance, while graphite filler worsens the wear resistance of the GF-epoxy	[20]
Cenospheres +Polyester	Open mould casting	10 wt.%	Submicron size cenospheres decreased the CoF and specific wear rate.	[30]
Cenospheres + vinyl ester	Open mould casting	10 wt. %	Submicron size cenospheres contributed to increase in the wear resistance	[31]
SiC, Al_2O_3, and ZnO particulates +novolac epoxy	Open mould casting	10 wt. % each	All micron size fillers show improved wear resistance and reduced CoF.	[32]
Graphite + epoxy	Open mould casting	10 wt.% (20 μ) 5 wt. % -(10 μ)	5 wt. % graphite reduced the CoF and enhanced the wear resistance.	[33]
Nano-Al_2O_3 +chopped carbon fiber + epoxy	Open mould casting	1, 2, 4 and 6 wt. % CF 4 wt.% CF + 1, 2, 3 and 4 wt. % Nano-Al_2O_3	CFs are very effective in reducing CoF Specific wear rate decreased by releasing a quantity of lubricant film on the counterface.	[34]
Nano-Al_2O_3, nano-SiO_2, nano-zirconia, gypsum micro-filler +Monomer resin BisGMA	Open mould casting	1, 2, 3 and 4 wt. % each	Addition of 3 wt.% of silane treated nano-silica in the dental composite evidenced effective for enhancing the wear resistance.	[35]
Nano-SiO_2 and carbon nanotubes + carbon-epoxy	Vacuum infusion process	0.1, 0.5 and 0.9 wt. % each	Both nano-particles improved friction coefficient and wear rates of carbon-epoxy	[36]
Glass fiber + epoxy	Hand lay-up	10 to 50 wt. % Short GF 10 to 50 wt. % Woven GF	Short GF-epoxy composites were found to exhibit higher wear resistance than that of the bidirectional GF-epoxy composites	[37]
E-glass fabric+ epoxy composites with and without graphite filler	Hand lay-up	2.5, 5 and 7.5 wt. %	Experimental result showed the following trend for abrasive wear rate: graphite filled GF-epoxy composites>GF-epoxy	[38]
SiC particulate + GF-epoxy	Hand lay-up	2.5, 5 and 7.5 wt. %	Experimental results showed the positive impact of SiC fillers, which enhanced the abrasive wear resistance of GF-epoxy composites	[39]

Several research looked at the use of micron-sized fillers to improve the abrasion resistance of polymer composites reinforced with glass fibre materials [20–24]. According to research by Hemanth et al., the specific wear rate of TCE + PTFE composite composites is high, but it can be decreased by adding micron-sized fillers (silicon carbide, pine bark dust) to the TCE + PTFE composite [25]. According to the study, Vikas sharma et al. [26] investigated whether adding fly ash improved the abrasion resistance of epoxy composites bonded with glass fibre. Kumaresan et al. [27] investigated the three-body abrasive wear behaviour of epoxy composites reinforced with carbon fabric. They found that incorporating micron-sized SiC particles into the same increases

its resistance to abrasion. The effects of TiO_2 and ZnO on the use of bidirectional glass reinforced polyester composites were examined by Singh et al. [28]. TiO_2-filled hybrid composites outperformed ZnO-filled hybrid composites in testing, the researchers found. The thermo-mechanical and wear characteristics of woven glass fibre composites that have silicon carbide incorporated were studied by Agarwal et al. [29]. The results showed a rising or falling trend as well as important components in each analysis. There was also discussion of the trend and key factors affecting the decrease in specific wear rate. Most recent literatures [17,20,30-39] on micro and nano sized fillers are provided in Table 1.

Hence, this study aimed to illustrate how different micron-sized fillers, including silicon dioxide, alumina, graphite, and fly ash cenosphere particulates, affected the behaviour of three-bodies of abrasive wear, in particular the specific wear rate of bidirectional glass fabric reinforced epoxy composites. For different abrading distances with a constant applied load and rubber wheel speed, the wear volume as well as specific wear rate was computed.

2. MATERIALS AND METHODS

Used materials are plain weave woven glass fabrics weighing 360 g/m^2 (E-glass) with fibre diameters ranging from 10 to 13 µm. LAPOX L-12 epoxy resin and K-6 hardener in a 100:12 weight ratio. Both materials were purchased by ATUL India Limited., Gujarat, India. Micron sized ceramic particles namely SiO_2, Al_2O_3, graphite (Gr), and fly ash cenosphere were collected from commercially available sources and used without further treatment. The average particle sizes of Al_2O_3, graphite, fly ash cenosphere and silica were20 µm, 25 µm, 32 µm and 25 µm respectively.

The hand lay-up method was used to create G-E composite laminates (200 mm × 200 mm × 10 mm) with and without ceramic fillers as listed in Table 2, which were then vacuum-bagged.

- Initially number of glass fabric layers required (55 wt. %) to achieve laminate thickness of 10 mm were cut for the dimension of 200 mm × 200 mm.
- Epoxy matrix along with hardener (35 wt. %) and micro sized fillers were mixed together thoroughly.
- First layer of the glass fabric was placed on the flat surface pre-cleaned with acetone.
- Epoxy mixture was then coated over the first layer with the help of a hand brush and thereafter second layer of the fabric was placed on the first layer.
- This process of applying the epoxy mixture and placing of new glass fabric layer was continued till desired thickness of 10 mm was measured.
- Air trapped between the layers of glass fibers were removed by placing the fabricated laminate in vacuum bag for 90 minutes duration.
- This was followed by curing the laminates at 120 °C for 120 min.

Table 2. Composite materials designations.

Composites	Alumina (wt.%)	Fly ash (wt.%)	Graphite (wt.%)	Silica (wt.%)
G-E	-	-	-	-
Alumina G-E	10	-	-	-
Fly ash G-E	-	10	-	-
Graphite G-E	-	-	10	-
Silica G-E	-	-	-	10

Table 3. Water jet machining parameters.

Parameter	Magnitude
Water pressure	200 MPa
Abrasive flow rate	300 g/min
Transverse speed	125 mm/min
Stand-off distance	1.5 mm

Laminates were then cut into the size of 75 mm x 25 mm x 10 mm for abrasion test with the help of water jet machining using cutting parameters provided in Table 3.

2.1 Three-body abrasion test

A diagrammatic representation of a Rubber wheel test rig is shown in Figure 1 and its specifications are provided in Table 4. The test samples are first weighed with a weighing balance machine (Make: Sartorius BSA224S-CW, Least Count: 0.0001 g) and their initial mass were noted (m_i).

Table 4. Specifications of rubber wheel test rig.

Parameter	Magnitude
Wheel diameter	228 mm
Rubber wheel thickness	12.7 mm
Wheel speed	200 rpm
Rubber hardness	60 Shore-D
Abrasive sand size	100-200 μm
Abrasive flow rate	350 g/min

The specimen is then put in the test setup's specimen holder, which is located across from the rubber wheel. The loads are then applied. The machine is then run by giving the test samples the required number of rotations, which causes abrasive sand particles to flow clockwise between the rubber wheel and the test sample. At that point, the test sample is being abraded as the wheel rotating at 200 rpm presses up against it and the sand flows downwards via nozzle at the rate of 350 g/min. The machine stops running after the specified number of revolutions, and the test sample is removed from the sample holder and weighed once more(m_f). This weight is then compared with the sample's initial weight(m_i), to find the wear mass loss($\Delta m=m_i-m_f$) and specific wear rate (SWR, also known as wear factor). The wear tests were conducted with two applied weights (20 N and 40 N), four abrading distances (500 m, 1000 m, 1500 m, and 2000 m), and a constant speed of 200 rpm.

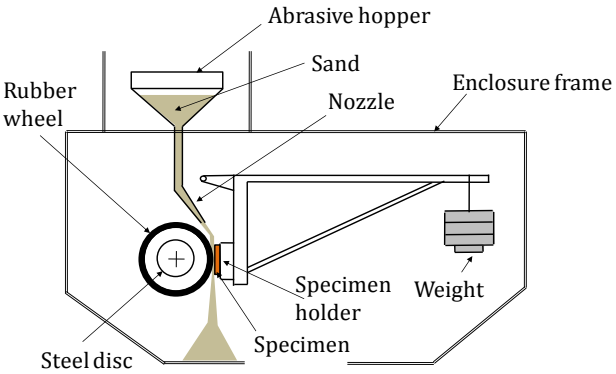

Fig. 1. Dry sand rubber wheel apparatus.

The calculation of the SWR or wear factor (K_s) is done as per ASTM G40 standard using the following equation:

$$K_s = \frac{\Delta V}{P \times D} \text{ (m}^3\text{/N m)} \quad (1)$$

where, ΔV represents the wear volume loss in m^3which is obtained by dividing the wear mass loss (Δm in gram) by the density (ρ in g/m^3) of corresponding composite samples i.e. ΔV=Δm / ρ as per ASTM G65;*P* represents the applied normal load in Newton and *D* represents the abrading distance in meters. The involved wear mechanisms of the selected abraded test samples were examined using a scanning electron microscope (SEM, Make: JEOL, JSM-IT300 series with magnification of x5-x300000).

3. RESULTS AND DISCUSSION

3.1 Effect of filler materials on wear volume

Wear volume loss versus abrading distance for G-E composites filled with various filler materials are shown in Figures 2 and 3 for applied normal loads of 20 N and 40 N, respectively. Compared to metals, polymer composites offer very less resistance to abrasion [40]. Hence, as recommended by ASTM G65 standard, light load variation from 20 N to 40 N was adopted for the conduction of wear tests.

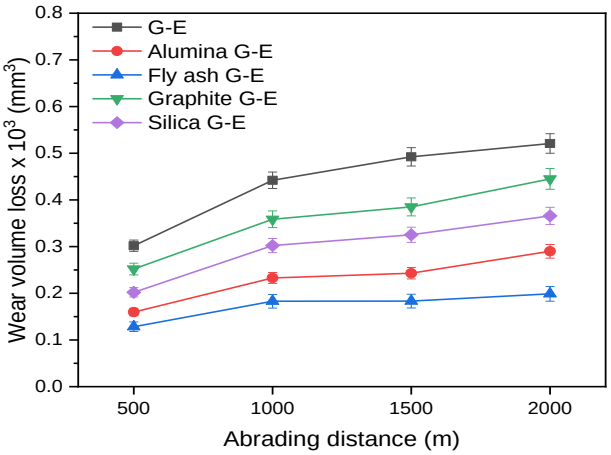

Fig. 2. Wear volume loss as a function of abrading distance of filled G-E composites at 20 N.

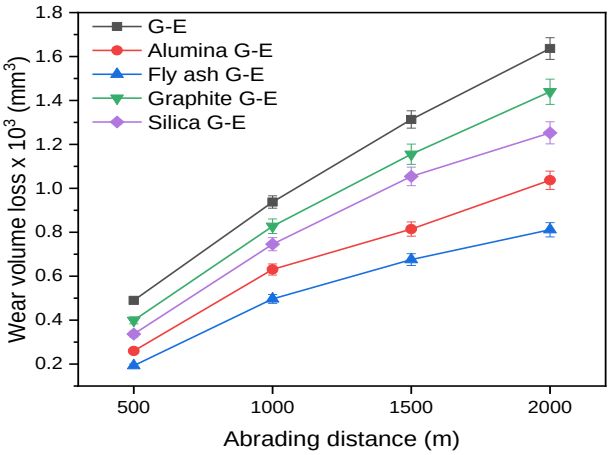

Fig. 3. Wear volume loss as a function of abrading distance of filled G-E composites at 40 N.

In the case of particulate filled G-E composites, fly ash cenosphere filled G-E showed lower wear volume performance. For almost all composite materials, wear volume has shown a saturation level after 1500 m abrading distance. The results in Figures 2 and 3 suggested that the ranking order of the abrasive wear performance of the composite materials changed on the abrading distance and applied normal load. Such variation in the abrasive wear performance depending on the abrading distance has also been reported by Suresha et al. [17,27,38]. Between 500 m and 2000 m of abrading distance were recorded while holding some tribo-variables constant (sliding speed:200 rpm, abrasive size: 225 μm). The figures 2 and 3 demonstrate that with increase in abrading distance, the wear volume steadily increases for all composites having the lowest wear volume loss at the lowest abrading distance of 500 m and the maximum wear volume loss at the highest abrading distance of 2000 m. Among all filled composites, fly ash cenosphere/G-E composites had the lowest wear volume loss of 0.128× 10^3 mm^3 at 20 N and 500 m abrading distance, while G-E epoxy composites had the highest wear volume loss. At applied loads of 20 N and 40 N, G-E composite with Al_2O_3had the second-lowest wear volume loss and SiO_2/G-E composites had the third-lowest wear volume loss as depicted in Figures 2 and 3 respectively.

3.2 Effect of filler materials on specific wear rate

Specific wear rate (SWR) versus abrading distance of G-E and their filler filled G-E composites are depicted in Figures 4 and 5. Figures 4 and 5 show an impact on SWR for Al_2O_3, fly ash cenospheres, SiO_2, and Gr particles filled G-E composites at 20 N and 40 N applied loads, respectively. At 20 N, the SWR gradually decreased as the abrading distance was increased, with the lowest SWR (0.232×10^{-11} $m^3N^{-1}m^{-1}$) for fly ash filled glass fabric reinforced epoxy composite at the highest abrading distance of 2000 m and the highest SWR ($3\times10^{-11}m^3N^{-1}m^{-1}$) for G-E composite at the smallest abrading distance of 500 m (Figure 4) at 20 N. The SWR of G-E composite varies between 3.386 ×10^{-11} $m^3N^{-1}m^{-1}$and 2.113×10^{-11} $m^3N^{-1}m^{-1}$with a load application of 40 N and at abrading distances of 500 m and 2000 m, respectively. Fly ash filled G-E composite has SWR values that range from 2.12×10^{-11} $m^3N^{-1}m^{-1}$to 1.21×10^{-11} $m^3N^{-1}m^{-1}$respectively. Al_2O_3 filled G-E composite has SWR values that range from 2.45×10^{-11} m^3 $N^{-1}m^{-1}$to 1.43×10^{-11} $m^3N^{-1}m^{-1}$, respectively.

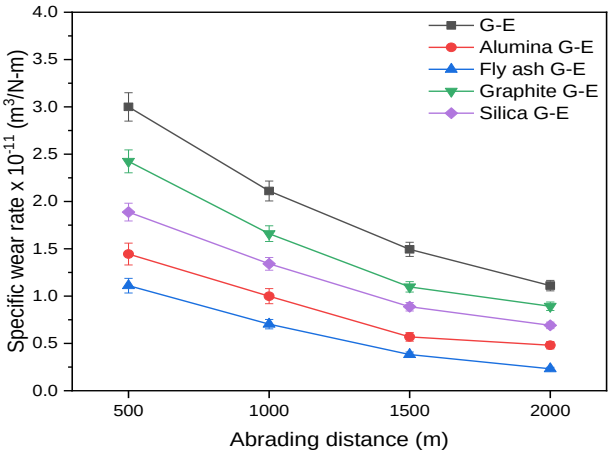

Fig. 4. SWR as a function of abrading distance for filled G-E composites at 20N.

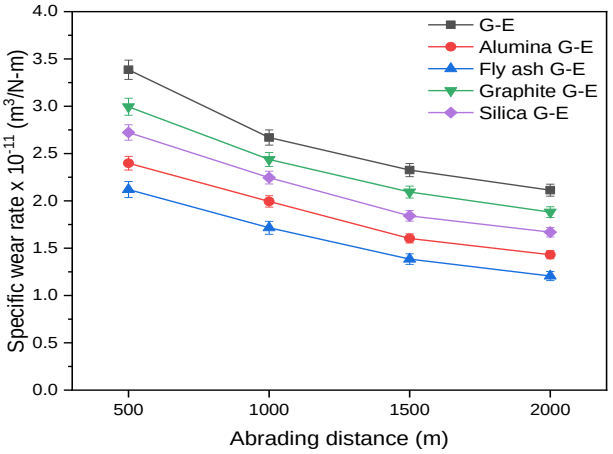

Fig. 5. SWR as a function of abrading distance for filled G-E composites at 40 N.

Furthermore, SiO_2/G-E composites have SWR values that range from 2.72×10^{-11} $m^3N^{-1}m^{-1}$ to 1.61×10^{-11} $m^3N^{-1}m^{-1}$, respectively. Gr filled G-E has SWR values that range from 2.99×10^{-11} $m^3N^{-1}m^{-1}$to 1.88×10^{-11} $m^3N^{-1}m^{-1}$, respectively.

The applied load of 40 N showed the same trend. Therefore, it can be inferred from the data that the SWR decreases as the abrading distance rises. The maximum SWR for G-E composites has been observed, as illustrated in Figures 6 and 7, when compared to filled G-E composite materials at 500 m abrading distance with 20 N and 40 N applied loads. Fly ash/G-E composite showed the least SWR as compared to other G-E and other filled G-E composites. The SWR in the descending order is as follows: G-E> Gr/G-E> SiO_2/G-E>Al_2O_3/G-E> Fly ash/G-E. When the different filler materials were added to G-E, it appeared better abrasion resistance. Therefore, it may be concluded that the SWR is deceased by the addition of fillers.

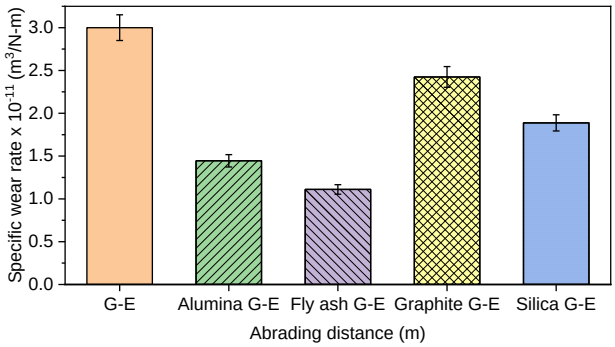

Fig. 6. SWR of filled G-E composites at 500m and 20N.

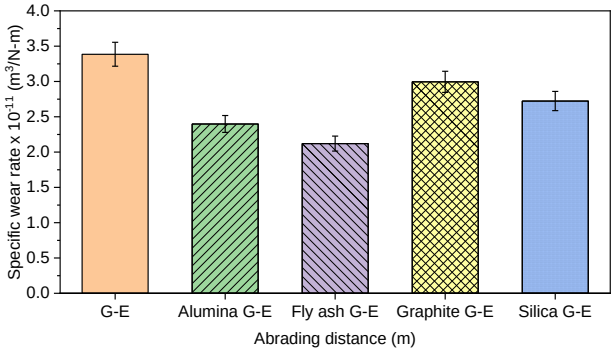

Fig. 7. SWR of filled G-E composites at 500m and 40N.

3.3 Worn surface morphology of filled G-E composites

Abrasive wear can be affected by several factors like the characteristic motion, surface properties and abrasion properties. Furthermore, abrasion mechanisms can be affected by range of particles size, particle, and surface component properties, contact pressure and velocity of the rubber wheel. The surface deformation depends on the constituents in the final composite. The worn out composite surfaces were gold sputtered by using the evaporation process with current 15 mA and voltage 1 kV for 10 minutes duration. The gold sputtering process was done to get the conductive coating of 750 Å over the worn surfaces, which is the prerequisite to get good quality SEM images.

As illustrated in Figure 8, G-E composite was tested at a normal load application of 40N and a worn surface at 2000 m. Figure 8 demonstrates that under a high applied load (40 N), the damage was more pronounced in the top/bottom resinous regions, with significant fibre degradation in the middle region. It is only possible to discern pitting (denoted by the letter "P") in the resinous areas and a network of micro cracks (denoted by the letter "M") in the vicinity of the bridging glass fibres. Only a few broken fibres were being dragged out, and the clean fibres looked to be intact in the abrading direction with a stepped appearance of glass fibres (marked "SA").

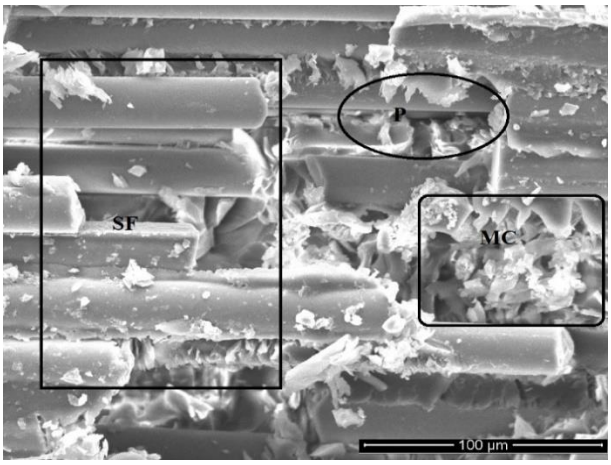

Fig. 8. Worn surface morphology of G-E composite.

3.4 Worn surface morphology of Gr/G-E composites

Figure 9 depicts the wear-out surface of a Gr/G-E composite that was tested at a load application of 40 N and 2000 m abrading distance. Figure 9 demonstrates that the epoxy graphite/matrix and fibre areas were both damaged at a high applied load (40 N).

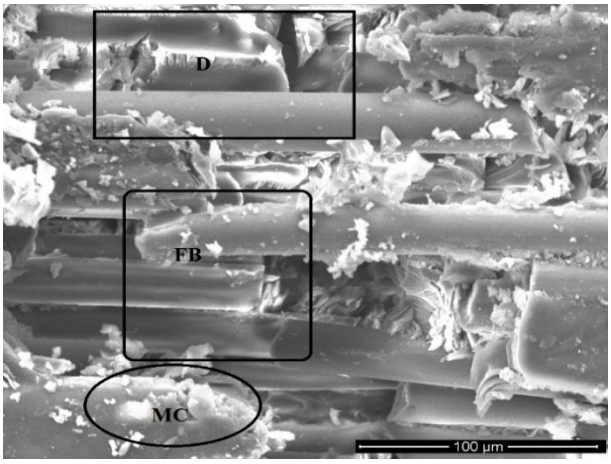

Fig. 9. Worn surface morphology of Gr/G-E composite.

Delamination (marked "D"), fibre breaking ("FB"), silica sand particles adhered to the epoxy matrix, and micro cracks of epoxy matrix ("MC") all happened. In addition, as shown in Figure 9, breakage occurred in the layered fabric, with broken fibres appearing to be worn-out, and a resinous layer of epoxy matrix with graphite particle pull-out occurred in the matrix/fabric interface region.

3.5 Worn surface morphology of SiO_2/G-E composites

Figure 10 depicts the wear-out surface of the SiO_2/ G-E composite that was evaluated at a 40 N load and 2000 m abrading distance. Figure 10's observations of a wear-out surface under higher applied load (40 N) show that the damage was most obvious in the fibrous region, where a large amount of the resinous region near the layers of glass fabrics had been lost. The particles were then encouraged to attack the fibres and cause damage as a result.

Additionally, as depicted in Figure 10, the stacked fibers fractured, resulting in the appearance of a steeped layer of broken fibres (designated "SA" in Figure 10) and a resinous layer of epoxy matrix with pull-out of silicon dioxide particles (designated "PO" in Figure 10).

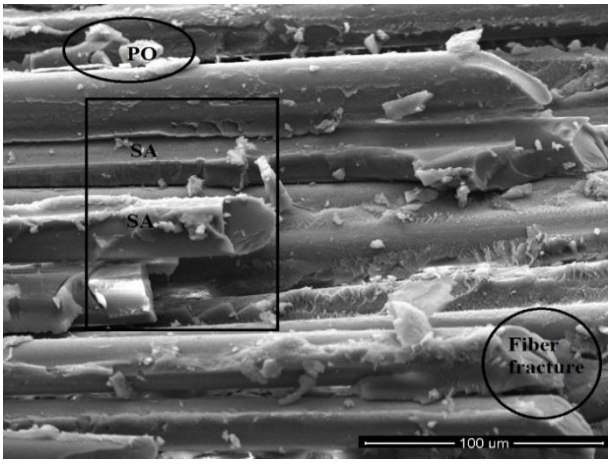

Fig. 10. Worn surface morphology of SiO_2/G-E composite.

3.6 Worn surface morphology of Al_2O_3/G-E composites

The wear behaviour of tribo-materials is sharply affected by the type, shape and size of the ceramic fillers. The presence of ceramic fillers like SiO_2 and Al_2O_3 in G-E composites changed the material surface characteristics by reducing voids and enhancing the structural integrity which resulted in increased abrasion resistance. Figure 11 depicts the wear-out surface of Al_2O_3 filled G-E composite tested at 40N applied normal load and 2000 m. The figure shows consistent thin resinous layer removal (marked "R") and strong bonding at the interface, which minimizes damage to the epoxy/ Al_2O_3 and glass fibres on the abraded composite surface.

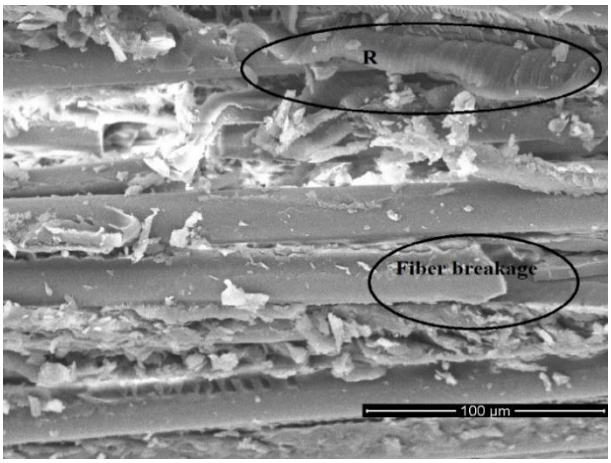

Fig. 11. Worn surface morphology of Al_2O_3/G-E composite.

This indicates that the silica sand fragments were not able to stick to the composite. When comparing the photomicrographs of G-E, Gr/G-E, and SiO_2/G-E composites from Figure 11, it could be inferred that there was only a very small amount of material present that caused less damage to the glass fibres, supporting the wear data.

3.7 Worn surface morphology of fly ash/G-E composite

Figure 12 depicts the worn surface of a fly ash filled G-E composite that was tested at a load application of 40N and 2000 m abrading distance. Less damage to the epoxy/fly ash and glass fibres on the abraded composite surface is seen in the image, i.e., uniform thin resinous layer removal (marked "R" in the picture) and strong bonding at the fiber/matrix interface. This indicates that silica sand fragments were not able to stick to composite.

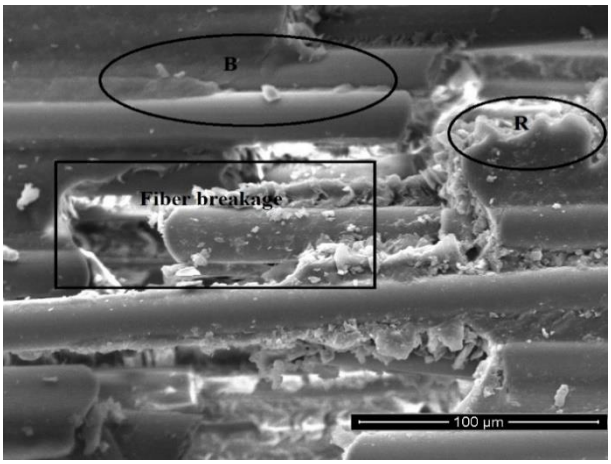

Fig. 12. Worn surface morphology of Fly ash/G-E composite.

Additionally, larger pieces of epoxy/fly ash particles were discovered on the surface, and the fibres seemed to be fractured but not debonded (indicated as "B"). This was accompanied in some places by little and large cracks, twisted grooves, and pitting. When comparing the photomicrographs of the unfilled Gr, SiO_2, and Al_2O_3 added G-E composites from Figure 12, it is reasonable to infer that there was only a very little amount of material, supporting the least specific wear rate, with less damage to both the matrix/fly ash and glass fibres.

4. CONCLUSIONS

In this investigation, G-E composites with and without ceramic fillers were made using by hand lay-up method followed by vacuum bagging. Three-body abrasive wear tests produced the following noteworthy results.

- Incorporation of fly ash cenosphere, Al_2O_3, SiO_2, and Gr micron-sized fillers into G-E composite revealed good performance in abrasive wear mode. The following factors were observed to be important in controlling the wear performance of the composites.
  - (i) All the fillers (irrespective of shape and size) used in the present work enhanced the epoxy matrix phase's interfacial bonding.
  - (ii) The applied load and abrading distance.
  - (iii) The extent of modification of the composite surface which reduced the wear rate in longer abrading distance run.
- Under all trio-test settings, the SWR for all particulate G-E composites decreases in the following order: G-E > Gr/G-E > SiO_2/G-E > Al_2O_3/G-E > fly ash cenosphere/G-E.
- Photomicrographs show various wear mechanisms of G-E with and without filler. The wear mechanisms involved are ploughing, fibre breakage, fibre pull-out, fibre thinning, and a network of microcracks.
- The fly ash cenosphere proved to be more wear resistant than Al_2O_3, SiO_2 and graphite.

REFERENCES

[1] A.G. Gibson, *Composite materials in the offshore industry,* Comprehensive Composite Materials vol. 6, pp. 459-478, 2000, doi: 10.1016/B0-08-042993-9/00115-7

[2] V. Fiore, G. Di Bella, A. Valenza, *Glass–basalt/epoxy hybrid composites for marine applications,* Materials & Design, vol. 32, iss. 4, pp. 2091-2099, 2011, doi: 10.1016/j.matdes.2010.11.043

[3] I.M. Hutchings, *Wear-resistant materials: into the next century,* Materials Science and Engineering: A, vol. 184, iss. 2, pp. 185-195,1994, doi: 10.1016/0921-5093(94)91031-6

[4] P. Panda, S. Mantry, S. Mohapatra, S.K. Singh, A. Satapathy, *A study on erosive wear analysis of glass fiber–epoxy–AlN hybrid composites,* Journal of Composite Materials, vol. 48, iss. 1, pp.107-118, 2014, doi: 10.1177/0021998312469239

[5] A.K. Rout, A. Satapathy, *Study on mechanical and tribo-performance of rice-husk filled glass–epoxy hybrid composites*, Materials & Design, vol. 41, pp. 131-141, 2012, doi: 10.1016/j.matdes.2012.05.002

[6] S.S. Moorthy, K. Manonmani, T. Elangovan, *An optimization approach to the dry sliding wear behavior of particulate filled glass fiber reinforced hybrid composites*, Journal of Engineered Fibers and Fabrics, vol. 10, iss. 2, pp. 113-120, 2015, doi: 10.1177/155892501501000213

[7] A.A Megahed, M.A. Agwa, M. Megahed, *Improvement of hardness and wear resistance of glass fiber-reinforced epoxy composites by the incorporation of silica/carbon hybrid nanofillers*, Polymer-Plastics Technology and Engineering, vol. 57, iss. 4, pp. 251-259, 2018, doi: 10.1080/03602559.2017.1320724

[8] B. Suresha, R.M. Devarajaiah, T. Pasang, C. Ranganathaiah, *Investigation of organo-modified montmorillonite loading effect on the abrasion resistance of hybrid composites*, Materials & Design, vol. 47, pp. 750-758, 2013, doi: 10.1016/j.matdes.2012.12.056

[9] R.K. Nayak, A. Dash, B.C. Ray, *Effect of epoxy modifiers (Al_2O_3/SiO_2/TiO_2) on mechanical performance of epoxy/glass fiber hybrid composites*, Procedia Materials Science, vol. 6, pp. 1359-1364, 2014, doi: 10.1016/j.mspro.2014.07.115

[10] J. Singh, M. Kumar, S. Kumar, S.K. Mohapatra, *Properties of glass-fiber hybrid composites: a review,* Polymer-Plastics Technology and Engineering, vol. 56, iss. 5, pp. 455-469, 2017, doi: 10.1080/03602559.2016.1233271

[11] R.S. Raja, K. Manisekar, V. Manikandan, *Study on mechanical properties of fly ash impregnated glass fiber reinforced polymer composites using mixture design analysis*, Materials & Design, vol. 55, pp. 499-508, 2014, doi: 10.1016/j.matdes.2013.10.026

[12] S. Nayak, R.K. Nayak, I. Panigrahi, A.K. Sahoo, *Tribo-mechanical responses of glass fiber reinforced polymer hybrid nanocomposites*, Materials Today: Proceedings, vol. 18, iss. 7, pp. 4042-4047, 2019, doi: 10.1016/j.matpr.2019.07.347

[13] M.D. Kiran, H.K. Govindaraju, T. Jayaraju, *Evaluation of mechanical properties of glass fiber reinforced epoxy polymer composites with alumina, titanium dioxide and silicon carbide fillers,* Materials Today: Proceedings, vol. 5, iss. 10, pp. 22355-22361, 2018, doi: 10.1016/j.matpr.2018.06.602

[14] T.A. Negawo, Y. Polat, Y. Akgul, A. Kilic, M. Jawaid, *Mechanical and dynamic mechanical thermal properties of ensete fiber/woven glass fiber fabric hybrid composites,* Composite Structures, vol. 259, iss. 1, pp. 113221, 2021, doi: 10.1016/j.compstruct.2020.113221

[15] M. Manjunath, N.M. Renukappa, B. Suresha, *Influence of micro and nanofillers on mechanical properties of pultruded unidirectional glass fiber reinforced epoxy composite systems*, Journal of Composite Materials, vol. 50, iss. 8, pp. 1109-1121, 2016, doi: 10.1177/0021998315588623

[16] B. Suresha, G.S. Divya, G. Hemanth, H.M. Somashekar, *Physico-mechanical properties of nano silica-filled epoxy-based mono and hybrid composites for structural applications*, Silicon, vol. 13, iss. 7, pp. 2319-2335, 2021, doi: 10.1007/s12633-020-00812-8

[17] B.N. Ramesh, B. Suresha, *Optimization of tribological parameters in abrasive wear mode of carbon-epoxy hybrid composites,* Materials & Design, vol. 59, pp. 38-49, 2014, doi: 10.1016/j.matdes.2014.02.023

[18] B.S. Kanthraju, B. Suresha, *Enhancement of mechanical properties and wear resistance of epoxy: glass fiber, basalt fiber, polytetrafluoroethylene and graphite*, Indian Journal of Advances in Chemical Science S1, pp. 107-113, 2016

[19] Y. Wang, O.I. Zhupanska, *Lightning strike thermal damage model for glass fiber reinforced polymer matrix composites and its application to wind turbine blades,* Composite Structures, vol. 132, pp. 1182-1191, 2015, doi: 10.1016/j.compstruct.2015.07.027

[20] B. Suresha, G. Chandramohan, P.V. Mohanram, *Role of fillers on three-body abrasive wear behavior of glass fabric reinforced epoxy composites,* Polymer Composites, vol. 30, iss. 8, pp. 1106-1113, 2009, doi: 10.1002/pc.20662

[21] B. Suresha, G. Chandramohan, T. Jayaraju, *Influence of cenosphere filler additions on the three-body abrasive wear behavior of glass fiber-reinforced epoxy composites,* Polymer Composites, vol. 29, iss. 3, pp. 307-312, 2008, doi: 10.1002/pc.20380

[22] B. Suresha, G. Chandramohan, *Three-body abrasive wear behaviour of particulate-filled glass–vinyl ester composites,* Journal of Materials Processing Technology, vol. 200, iss. 1-3, pp. 306-311, 2008, doi: 10.1016/j.jmatprotec.2007.09.035

[23] B. Suresha, G. Chandramohan, M. Abraham Jawahar, S. Mohanraj, *Three-body abrasive wear behavior of filled epoxy composite systems,* Journal of Reinforced Plastics and Composites, vol. 28, iss. 2, pp. 225-233, 2009, doi: 10.1177/0731684407084247

[24] K.M. Subbaya, B. Suresha, N. Rajendra, Y.S. Varadarajan, *Taguchi approach for characterization of three-body abrasive wear of carbon-epoxy composite with and without SiC filler,* Composite Interfaces, vol. 19, iss. 5, pp. 297-311, 2012, doi: 10.1080/15685543.2012.720903

[25] H. Rajashekaraiah, S. Mohan, P.K. Pallathadka, B. Suresha, *Dynamic mechanical analysis and three-body abrasive wear behaviour of thermoplastic copolyester elastomer composites.* Advances in Tribology, vol. 2014, pp. 1-14, 2014, doi: 10.1155/2014/210187

[26] V. Sharma, M.L. Meena M. Kumar, *Effect of filler percentage on physical and mechanical characteristics of basalt fiber reinforced epoxy based composites,* Materials Today: Proceedings, vol. 26, pp. 2506-2510, 2020, doi: 10.1016/j.matpr.2020.02.533

[27] K. Kumaresan, G. Chandramohan, B. Suresha, *Dynamic mechanical analysis and three-body wear of carbon–epoxy composite filled with SiC particles,* Journal of reinforced Plastics and Composites, vol. 31, iss. 21, pp. 1435-1448, 2012, doi: 10.1177/0731684412459250

[28] A.K. Singh, , Siddhartha, Deepak, *Assessment of mechanical and three-body abrasive wear peculiarity of TiO_2- and ZnO-filled bi-directional E-glass fibre-based polyester composites,* Bulletin of Materials Science, vol. 39, pp. 971–988, 2016, doi: 10.1007/s12034-016-1237-4

[29] G. Agarwal, A. Patnaik, R.K. Sharma, *Thermo-mechanical properties and abrasive wear behavior of silicon carbide filled woven glass fiber composites,* Silicon, vol. 6, iss. 3, pp. 155-168, 2014, doi: 10.1007/s12633-014-9184-4

[30] A.K. Singh, Siddhartha, *Leverage of cenosphere filler size on mechanical and dry sliding wear peculiarity of polyester composites,* Journal of Composite Materials, vol. 49, iss. 22, pp. 2789-2802, 2015, doi: 10.1177/0021998314554436

[31] S. Thakur, S. Chauhan, *Effect of micron and submicron size cenosphere particulate on mechanical and tribological characteristics of vinyl ester composites,* Proceedings of the Institution of Mechanical Engineers, Part J: Journal of Engineering Tribology, vol. 228, iss. 4, pp. 415-423, 2014, doi: 10.1177/1350650113513444

[32] K. Dass, S.R. Chauhan, B. Gaur, *Effects of microsize SiC, Al_2O_3, and ZnO particulates on mechanical and tribological properties of synthesized ortho-and meta-cresol novolac epoxy composites,* Proceedings of the Institution of Mechanical Engineers, Part J: Journal of Engineering Tribology, vol. 228, iss. 8, pp. 881-895, 2014, doi: 10.1177/1350650114535570

[33] N. Gafsi, I. Smaoui, R. Verdejo, M. Kharrat, M.A. Manchado, M. Dammak, *Tribological and mechanical characterization of epoxy/graphite composite coatings: Effects of particles' size and oxidation*, Proceedings of the Institution of Mechanical Engineers, Part J: Journal of Engineering Tribology, vol. 235, iss. 1, pp. 129-137, 2021, doi: 10.1177/1350650120944273

[34] K. Dass, S.R. Chauhan, B. Gaur, *Study on the effects of nano-aluminium oxide particulates on mechanical and tribological characteristics of chopped carbon fiber reinforced epoxy composites*, Proceedings of the Institution of Mechanical Engineers, Part L: Journal of Materials: Design and Applications, vol. 231, iss. 4, pp. 403-422, 2017, doi: 10.1177/1464420715598798

[35] S.R. Kumar, A. Patnaik, I.K. Bhat, T. Singh, *Optimum selection of nano-and micro sized filler for the best combination of physical, mechanical, and wear properties of dental composites*, Proceedings of the Institution of Mechanical Engineers, Part L: Journal of Materials: Design and Applications, vol. 232, iss. 5, pp. 416-428, 2018, doi: 10.1177/1464420716629825

[36] M.R. Ayatollahi, R. Moghimi Monfared, R. BarbazIsfahani, *Experimental investigation on tribological properties of carbon fabric composites: effects of carbon nanotubes and nano-silica*, Proceedings of the Institution of Mechanical Engineers, Part L: Journal of Materials: Design and Applications, vol. 233, iss. 5, pp. 874-884, 2019, doi: 10.1177/1464420717714345

[37] G. Agarwal, A. Patnaik, R.K. Sharma, *Comparative investigations on three-body abrasive wear behavior of long and short glass fiber-reinforced epoxy composites*, Advanced Composite Materials, vol. 23, iss. 4, pp. 293–317, 2014, doi: 10.1080/09243046.2013.868661

[38] B. Suresha, G. Chandramohan, Siddaramaiah, *Three body abrasive wear behavior of E-glass fiber reinforced/graphite-filled epoxy composites*, Polymer Composites, vol. 29, iss. 6, pp. 631–637, 2008, doi: 10.1002/pc.20447

[39] B. Suresha, G. Chandramohan, P. Sampathkumaran, S. Seetharamu, *Mechanical and three-body abrasive wear behaviour of SiC filled glass-epoxy composites*, Polymer Composites, vol. 29, iss. 9, pp. 1020-1025, 2008, doi: 10.1002/pc.20576

[40] M. Qian, P. Song, Z. Qin, S. Yan, L. Zhang, *Mechanically robust and abrasion-resistant polymer nanocomposites for potential applications as advanced clearance joints*, Composites Part A: Applied Science and Manufacturing, vol. 126, p. 105607, 2019, doi: 10.1016/j.compositesa.2019.105607